Annotated Revised Manuscript

On the Use of the Frequency Domain in Assessing Resonant Overvoltages during Transformer Energization

Willem Leterme, Evelyn Heylen and Dirk Van Hertem

***Abstract*—Resonant temporary overvoltages during transformer energization may result in damage to the transformer itself or surrounding equipment. These overvoltages are caused by the interplay between the transformer energization currents and the grid impedance. Current practice to assess the risk of transformer energization is by classifying grid scenarios into potentially problematic or non-problematic based on the magnitude of the grid impedance at frequencies coinciding with the grid harmonic frequencies. At the moment, this approach lacks a proof of validity. Therefore, this paper investigates the use of frequency-domain characteristics, and more in general, linear analysis of the grid impedance, for assessing the risk associated with transformer energization. Findings show that the magnitude of the frequency domain grid impedance may not provide sufficient information for classifying problematic and non-problematic cases.**

I. Introduction

Overvoltages during transformer energization may be caused by resonance phenomena when energizing a transformer in the presence of underground cables in the power system [1]. These overvoltages, called resonant Temporary OverVoltages (TOV) may be harmful to, and potentially cause failure of, the transformer itself or other components such as surge arresters. Before switching in a transformer or applying autoreclosure schemes in the vicinity of a transformer, it is therefore crucial to assess the risk of potential harmful overvoltages, as e.g., proposed in [2–4].

To avoid the computational burden of a time-domain analysis per transformer energization event, system operators resort to frequency domain analysis of the grid impedance [2], [4]. A frequency domain analysis on the grid impedance involves calculating the magnitude of the grid impedance for frequencies coinciding with harmonic frequencies (e.g. 100-150-200 Hz) and comparing these against a pre-set threshold. The pre-set threshold is, e.g., for each frequency of interest, calculated using a time-domain analysis of an RLC circuit with a resonance at that frequency [2], [5], or based on experience [4]. Only for those grid situations in which the magnitude of the grid impedance exceeds the pre-set threshold, the frequency domain analysis is complemented by a time-domain analysis. At present, transmission system operators (TSOs) use different thresholds in the frequency domain to distinguish problematic from non-problematic cases (Table I). There is at present little information on how these thresholds are determined.

TABLE I: Frequency domain thresholds as used by TSOs

RTE	300 Ω @ f=100 Hz [2]
EnergiNet	400 Ω @ f=100 ±10 Hz [4]
EirGrid	1000 Ω ∀ f < 150 Hz [6]

This paper investigates the suitability of frequency-domain analyses in assessing the risk of transformer energization. In particular, this paper assesses the use of the magnitude of the grid impedance as a feature for classifying transformer energization events into problematic or non-problematic. Therefore, this paper first discusses the approach of [7] for assessing risks associated with transformer energization (Section II). Then, it recapitulates the basic features of two example RLC-circuits, which can be used to mimic a grid impedance with a resonance, in frequency and Laplace domain (Section III). Finally, it analyzes the use of frequency domain characteristics for classifying transformer energization scenarios in a case study using these example circuits (Section IV).

II. Transformer Energization Failure Analysis

The analysis of failure during transformer energization is a nonlinear and stochastic problem. The nonlinearity is introduced by the transformer saturation, which links the transformer currents to the voltages at its terminals. The stochasticity is introduced by the uncertainty on the transformer residual flux, breaker switching instant and air core reactance [7]. Below, the procedure for analyzing transformer energization failure of [7] is introduced and discussed.

A. Procedure of [7]

The procedure aims at calculating the failure probability during transformer energization, p_f. To do so, the procedure uses a function g to calculate transformer stresses based on voltage waveforms during a simulated energization event. Using a threshold on g, this function is transformed into an indicator function ξ, which takes a value 1 for failure of a scenario and 0 otherwise. The aim of the procedure is to

This work received the support of the Energy Transition Funds funded by the FPS Economy, Belgium.

W. Leterme and D. Van Hertem are with KU Leuven, Belgium (EnergyVille/Electa research group, Electrical Engineering Department ESAT, Kasteelpark Arenberg 10 (PB2445), 3001 Heverlee).

E. Heylen is with Imperial College London (the Department of Electrical and Electronic Engineering, Imperial College, London SW7 2AZ, U.K.)

willem.leterme@esat.kuleuven.be

Paper submitted to the International Conference on Power Systems Transients (IPST2021) in Belo Horizonte, Brasil, June 6-10, 2021.

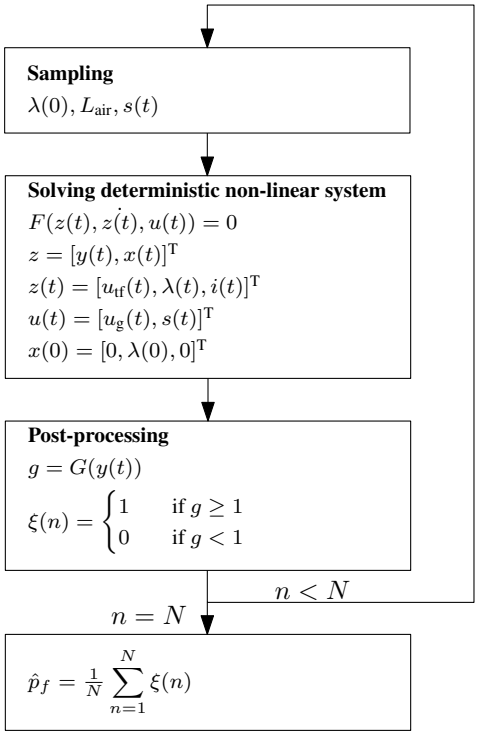

Fig. 1: Diagram for procedure of [7]

estimate the probability of failure of the transformer, or the expected value of the random variable Ξ, of which ξ represents one realization.

To estimate the probability of failure during transformer energization for a given grid impedance, the procedure uses a Monte Carlo method: (1) scenario sampling, (2) solving the deterministic non-linear system in the time domain using EMT-type software, (3) post-processing of the results to obtain an estimate of the probability of failure (Fig. 1).

1) Scenario sampling: Scenarios for transformer energization are sampled from the probability distributions of the residual flux $\lambda(t = 0)$ or $\lambda(0)$, air core reactance L_{air} and switching times $s(t)$. The equations and distributions for generating the samples are given in [7].

2) Time domain solution: Switching in a transformer (in the example electrical circuit shown in Fig. 2) with initial conditions and fixed parameters can be considered as a deterministic non-linear problem. The electrical circuit represents a transformer energized by a grid (in the example represented by a voltage source with voltage $u_{\text{g}}(t)$) through a frequency-dependent grid impedance Z_g. This frequency-dependent grid impedance can be a full-detailed electrical circuit representing the power system, or a frequency-dependent impedance based on a fit of that circuit. This problem is typically solved using EMT-type software, and gives a solution for the voltage at the transformer, $u_{\text{tf}}(t)$.

3) Post-processing: The post-processing step transforms the voltage waveforms into an indicator of stress for the transformer or other equipment. In [7], the use of a voltage-duration or U-t-curve is suggested. Such a curve relates the voltages on the equipment to the time that the equipment can

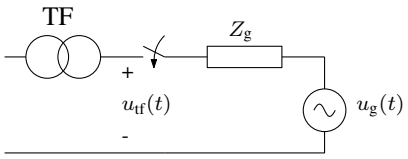

Fig. 2: Example electrical circuit for transformer energization

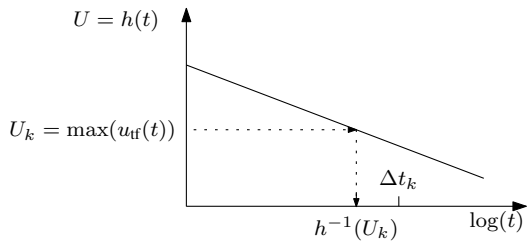

Fig. 3: Example voltage-duration curve.

withstand such a voltage. An example voltage-duration curve, based on the one suggested in [7] is given by:

$$h(t) = A \left(\frac{10}{t} \right)^{B} U_{\text{r}}, \tag{1}$$

where A and B are constants and U_{r} is the equipment's rated voltage. An example of such a curve is shown in Fig. 3.

In the post-processing step, the transformer voltages are used to calculate a "global-stress-rate" g. For a selection of time windows Δt_k, the maximum voltage U_k is calculated. This maximum voltage is used to calculate a maximum allowed time, by taking an inverse of the voltage-duration curve, i.e. $t_k = h^{-1}(U_k)$. The global stress rate g is then calculated as (similar to Miner's rule):

$$\begin{aligned} g &= \sum_{k=1}^{K} \frac{\Delta t_k}{h^{-1}(U_k)} \qquad , \\ U_k &= \max u_{\text{tf}}(t), \qquad t \in \Delta t_k, \end{aligned} \tag{2}$$

where $u_{\text{tf}}(t)$ is the voltage across the transformer terminals. A graphical example of (2) is given in Fig 3. It is important to note that there are at present questions with the use of this stress rate calculation. As indicated in the original paper [8], the above stated curves are built for fundamental frequency waveforms but used here in the context of waveforms containing not only fundamental but also harmonic frequencies. This is an ongoing topic of research, but is not within the scope of this paper.

To assess the probability by which g has exceeded 1, the cumulative distribution function of g, $F(g)$ can be approximated by the empirical cumulative distribution function $\hat{F}_N(g)$:

$$\hat{F}_N(g) = \frac{1}{N} \sum_{n=1}^{n=N} 1_{G \leq g}. \tag{3}$$

The probability of failure associated with $g_{\text{thr}} = 1$ is then given by $\hat{p}_f = 1 - \hat{F}_N(1)$.

B. Challenges and Workarounds

The challenges with respect to the above procedure lie in a potentially large execution time. The procedure may have a

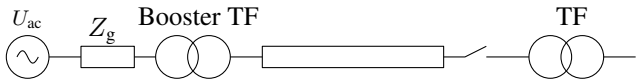

Fig. 4: Energization of a transformer radially connected to the grid via a cable.

large execution time because of two reasons. Solving the electrical circuit using EMT-type software may require a long time for extensive high-voltage systems. Given that the frequency of interest is relatively low (e.g. 100-200 Hz), an extensive part of the system must be modeled to achieve a reasonable accuracy. Even when using fitted macromodels to improve computational efficiency for simulating one transformer energization scenario, e.g., done in [9], the entire procedure still requires simulation of a large number of scenarios. This is due to the use of the Monte Carlo method, which typically requires a large number of scenarios before reaching convergence.

To avoid repeating the procedure described above for every grid situation, a common workaround is to resort to a binary classification of grid situations for transformer energization into problematic and non-problematic cases. The feature selected for the classification is the magnitude of the frequency-dependent grid impedance at harmonic frequencies such as 100, 150 and 200 Hz, or bands around these frequencies [4].

Calculating a threshold for the binary classification based on the grid impedance magnitude may in itself pose a challenge. In [2], RLC-circuits are used to calculate the thresholds for the classification of grid situations. These RLC-circuits are tuned such that the resonance frequency coincides with the harmonic frequency at which the threshold is calculated. A threshold for a given probability of failure, say $p_{\text{f,thr}}$ is found by applying the procedure described above to the RLC-circuits and increasing its magnitude at resonant frequency until the obtained probability of failure during transformer energization exceeds $p_{\text{f,thr}}$. The magnitude found then serves as boundary to determine non-problematic (grid impedances with lower magnitude at that frequency) from problematic cases (grid impedances with higher magnitude at that frequency).

In [5], thresholds are determined for the energization of an offshore transformer by an onshore grid through a submarine cable. In the particular situation, the cable is connected to the onshore grid by a booster transformer, which regulates the voltage (Fig. 4). For setting up a threshold for binary classification, the grid is simplified to the system shown in Fig. 5a. In this figure, L and R represent the combined grid short-circuit and booster transformer impedance and C represents the cable capacitance. From the viewpoint of the offshore transformer, this circuit represents a resonant circuit, with a parallel connection of C and the series connection of R and L. The procedure to set up the threshold in [5] is as follows: L is first fixed up-front according to the system's short-circuit impedance, C is then set such that the resonance frequency of the RLC-circuit coincides with the desired harmonic and R is finally varied to find the threshold on the impedance magnitude.

The remainder of the paper focuses on the suitability of the magnitude of the grid impedance as feature for classifying

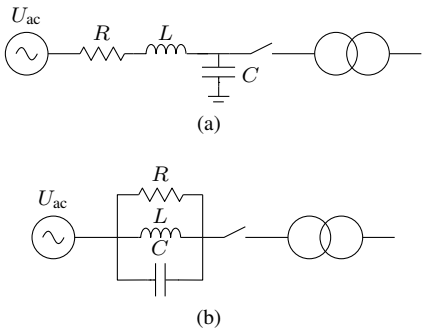

Fig. 5: Electrical circuit for transformer energization analysis; RL//C (a) and parallel RLC (b).

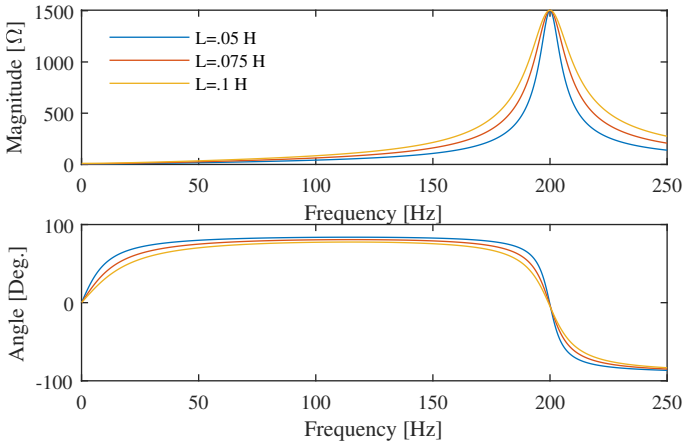

Fig. 6: Frequency response of example RL//C circuits.

transformer energization scenarios and the practical aspects with RLC-circuits to obtain thresholds.

III. RLC-circuits as representation of Z_G

This section discusses the basic characteristics of parallel RLC circuits in Laplace and frequency domains. The characteristics of these RLC circuits, e.g., the magnitude of the frequency-domain response at a certain frequency, are typically used to classify potentially problematic or non-problematic scenarios.

A. RLC-circuits with RL in parallel with C (RL //C)

The impedance of the RLC-circuit used in [5] is given in the Laplace domain by:

$$Z(s) = \frac{R + Ls}{LCs^2 + RCs + 1}. \tag{4}$$

For small R, the natural frequency is given by $\omega_n = 1/\sqrt{LC}$ and the magnitude at that frequency is given by $|Z(\omega_n)| \approx (\omega_n^2 L^2)/R$. For a given L, ω_n and $|Z(\omega_n)|$, the values for C and R can be derived.

Assuming three different values for L, the impedance in the frequency domain is given in Fig. 6 and the poles and zeros of (4) are given in Fig. 7. It can be seen that for an increase in L, the quality factor of the circuit decreases and the damping factor increases.

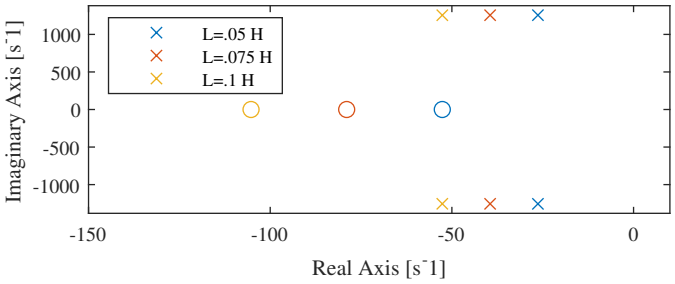

Fig. 7: Pole-zero map of example RL //C circuits.

B. Parallel RLC-circuit

Another approach to introducing a parallel resonance in the transformer energization problem is by using a parallel RLC-circuit. For a parallel RLC-circuit, the impedance $Z(s)$ is given in the Laplace domain by

$$Z(s) = LR\frac{s}{RLCs^2 + Ls + R}. \tag{5}$$

The natural frequency of the circuit is given by $\omega_n = \frac{1}{\sqrt{LC}}$ and the damping factor is $\zeta = \frac{1}{2\omega_n RC}$. If the RLC circuit is expressed in function of the quality factor Q, we obtain $\zeta = \frac{1}{2Q}$. From these values, we can calculate the time constant of the circuit, τ as $\tau = \frac{1}{\omega_n \zeta}$.

When evaluating the impedance of the RLC-circuit in the frequency domain, we obtain the following for the amplitude and the phase shift:

$$\begin{aligned} |Z(j\omega)| &= \frac{\omega RL}{\sqrt{R^2(1-\omega^2 LC)^2 + \omega L^2}}. \\ \angle Z(j\omega) &= 90 - \arctan\frac{\omega L}{R(1-\omega^2 LC)}. \end{aligned} \tag{6}$$

It can be seen that at the resonance point, the amplitude takes the value of R and the phase shift takes a value of 0, corresponding to the expected values for resistive behavior at the resonance point.

For using a parallel RLC circuit, one can choose L according to the short-circuit impedance of the system, and then choose C and R to obtain the desired resonance frequency and grid impedance magnitude at that resonance frequency.

Assuming the same three values for L as in the previous section, the impedance in the frequency domain is given in Fig. 8 and the poles and zeros of (5) are given in Fig. 9. Similar to the previous circuit, for an increase in L, the quality factor of the circuit decreases and the damping factor increases.

IV. Case Study

A case study is performed to analyze the suitability of the magnitude of the grid impedance as feature to classify grid situations with respect to resonant TOVs. The case study considers the energization of a transformer (with parameters given in Table II) through both RLC-circuits, given in Fig. 5a and b. In the case study, the RLC-circuits' resistance is considered to be 1500 Ω and three cases are considered for the inductance representing the grids' short-circuit impedance, i.e., $L = .05$ H, $L = .075$ H and $L = .1$ H.

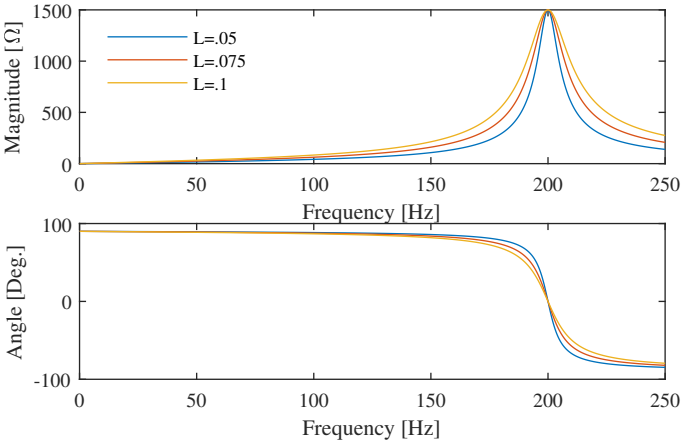

Fig. 8: Frequency response of example RLC circuits.

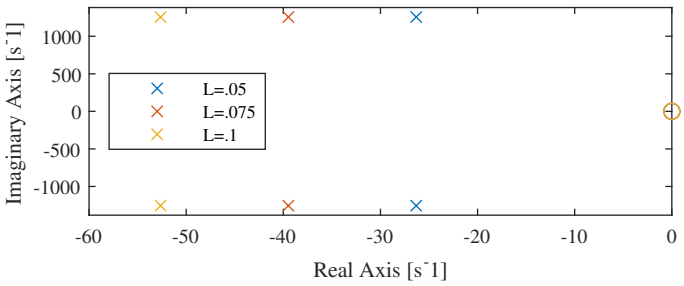

Fig. 9: Pole-zero map of example RLC circuits.

The case study makes use of the procedure described in Section II-A to analyze the transformer stresses. First, the Monte Carlo method generates $N = 301$ voltage waveforms for different scenarios of the remanent flux, air core reactance and breaker opening times are varied as outlined in [7]. Thereafter, the transformer's phase-to-phase voltages are analyzed using the U-t-curve as given by (1). The number of scenarios in the Monte Carlo method was kept intentionally low, as result outcomes are only used for demonstration purposes.

To determine the transformer stress using a U-t-curve (cf. Section IIA), a case resembling the curves in [7] is studied, with $[A, B] = [1.1892, .0388]$ (Fig 10). The global stress rate g is calculated using $[\Delta t_1, \Delta t_2, \Delta t_3, \Delta t_4] = [10e-3, 10e-2, 1, 2]$ s (cf. Section IIA).

The electrical circuit used for the transformer energization studies (Fig. 5) is modeled and solved in EMT-type software [10]. The transformer is modeled based on the classical modeling approach, where saturation is modelled across the magnetizing inductance [10]. The breakers are modeled as on-off resistances using $R_{\text{on}} = 0.005$ Ω and $R_{\text{off}} = 10^8$ Ω. The simulation timestep is set to 50 μs and the output timestep is 250 μs.

A. Results

1) RL//C circuit: Although the frequency domain magnitude is the same, the transformer failure probabilities for different values of L are widely different (Fig. 11). After 300 simulations, the Monte Carlo method converges to different values of $\hat{p}_f$, where the lowest $\hat{p}_f$ is associated with the largest

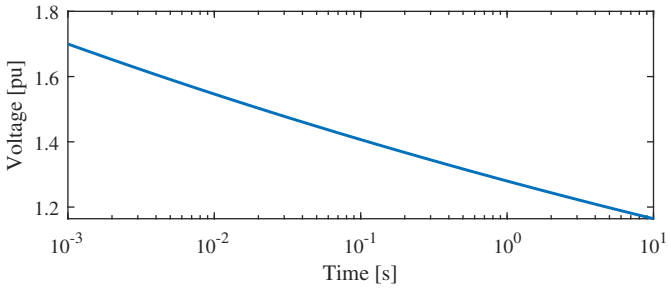

Fig. 10: U-t-curve for case study

TABLE II: Transformer Parameters

Parameter	Value
Rated Power	500 MVA
Primary Winding Voltage	380 kV
Secondary Winding Voltage	220 kV
Winding configuration	Star(g)-star(g)
Leakage reactance	0.18 pu
Winding losses	.01 pu
Base Air Core Reactance	0.3 pu
Magnetizing Current	0.1%
Knee Voltage	1.15
Loop width	10

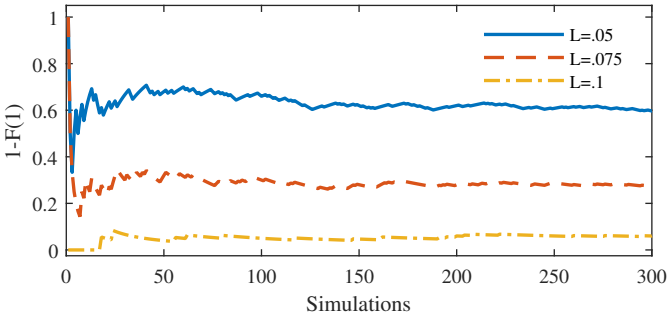

Fig. 11: Convergence of Monte Carlo method for the RL//C circuit.

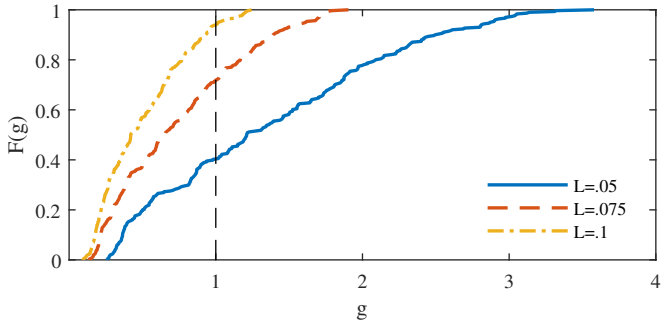

Fig. 12: Empirical cumulative distribution function of global stress rate for RL//C circuit.

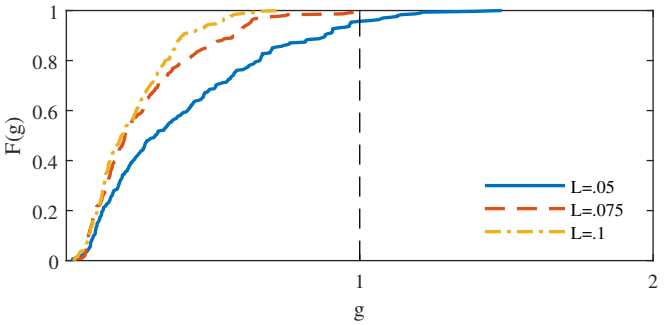

(a)

Fig. 13: Empirical cumulative distribution function of global stress rate for parallel RLC-circuit.

value of L. This may be surprising as one tends to associate the lowest short-circuit impedance (largest L) to the worst case scenarios. In the empirical cumulative distribution function, it can be seen that the lowest value of L also leads to the largest spread on g. This may be attributed to the fact that the largest L also coincides with the largest damping factor of the RL//C circuit, although further research is needed to draw firm conclusions. In any case, whenever the variation of L is large, the value of L should be accounted for when considering transformer energization in this type of circuits.

2) RLC circuit: As for the RL//C-circuit, the empirical cumulative distribution functions of the global stress rate show large differences (Fig. 13). The circuits associated with the largest L entail the lowest probability of failure for the same $|Z_{\max}|$. This fact could again be explained by the higher damping factor of the grid impedance for higher L, but further research is needed to confirm these conclusions. Even though the frequency domain characteristics are similar, the results obtained with this circuit are, as expected, not comparable to those obtained with the RL//C circuit. Although a parallel resonance can be exactly tuned using R and C, there is no link of the RLC circuits elements to physical grid behavior except when L is linked to the grid's short-circuit impedance.

V. Conclusion

Although the frequency-domain characteristics of the grid impedance may indicate potential harmful transformer energization scenarios, it is difficult to derive firm thresholds to classify problematic and non-problematic scenarios using only the magnitude of the impedance. This paper has used two types of RLC-circuits as equivalent grid representations to show that the failure probability of transformer energization not only depends on the magnitude of the impedance at resonance frequency, but also on other aspects such as the damping factor of the circuit. The two types of RLC-circuits considered in this paper are a series connection of a resistor and inductor, in parallel with the capacitor, and a parallel RLC-circuit. Demonstration cases for both circuits have shown that, even if the magnitude of the RLC-circuits impedance at a resonance frequency is the same, the probability of failure of a transformer energization differs and moreover depends on the variations in the inductance, and consequently the damping of the circuit. Future research may therefore focus on finding additional features that can be used to characterize grid situations with respect to resonant temporary overvoltages during transformer energization.

References

[1] M. Martinez-Duro, F.-X. Zgainski, and B. Caillault, "Transformer Energization Studies with Uncertain Power System Configurations," in *Proc.*

IPST 2013, Vancouver, Canada, Jul. 2013.
[2] Y. Vernay, S. Deschanvres, and Y. Fillion, "RTE experiences with the insertion of long EHVAC insulated cables," in *Proc. CIGRE 2014*, Paris, France, Aug. 2014.
[3] N. Cunniffe, M. Val Escudero, A. Mansoldo, E. Fagan, M. Norton, and C. Ellis, "Investigating the Methodology and Implications of Implementing Long HVAC Cables in the Ireland and Northern Ireland Power System," in *Proc. CIGRE 2016*, Paris, France, Aug. 2016.
[4] Energinet, "Technical Issues Related To New Transmission Lines in Denmark," Tech. Rep. Doc. 18/04246-24, Sep. 2018.
[5] S. Deschanvres and Y. Vernay, "Transient Studies performed by RTE for the connection of offshore wind farms," in *Proc. IPST 2013*, Vancouver, Canada, Jun. 2013.
[6] C. Ellis, "AC CABLE STUDIES FOR GRID WEST- Full and Partial AC Underground Solution," Staines-upon-Thames, UK, Tech. Rep. 10344 – PSP019, Jan. 2015.
[7] CIGRE WG C4.307, "Transformer Energization in Power Systems: A Study Guide," CIGRE, Tech. Rep. 568, 2014.
[8] CIGRE WG 33.10, "Temporary overvoltage withstand characteristics of extra high voltage equipment." *CIGRE Electra*, no. 179, Aug. 1998.
[9] Y. Vernay and B. Gustavsen, "Application of Frequency-Dependent Network Equivalents for EMTP Simulation of Transformer Inrush Current in Large Networks," in *Proc. IPST 2013*, Vancouver, Canada, Jun. 2013.
[10] PSCAD, *User's Guide - A comprehensive resource for EMTDC*. Manitoba HVDC Research Centre, 2018. [Online]. Available: https://www.pscad.com/uploads/knowledge_base/emtdc_manual_v4_6.pdf